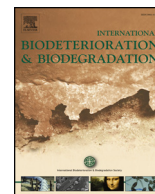




Contents lists available at ScienceDirect

International Biodeterioration & Biodegradation

journal homepage: www.elsevier.com/locate/ibiod

Antifouling properties of different Plasma Electrolytic Oxidation coatings on 7075 aluminium alloy



Pietrogianni Cerchier^{a,*}, Luca Pezzato^a, Emanuela Moschin^b, Leonardo Bertolucci Coelho^c, Marie Georges Marjorie Olivier^c, Isabella Moro^{b,**}, Maurizio Magrini^a

^a Department of Industrial Engineering, University of Padova, via Marzolo 9, 35131, Padova, Italy

^b Department of Biology, University of Padova, Via U. Bassi, 58/B, 35121, Padova, Italy

^c Department of Materials Science, Faculty of Engineering, University of Mons, 20 Place du Parc, 7000, Mons, Belgium

ARTICLE INFO

Keywords:

Antifouling
Plasma Electrolytic Oxidation (PEO)
Copper
Silver
Coating
Diatoms
SVET

ABSTRACT

In this work the antifouling properties of different Plasma Electrolytic Oxidation (PEO) coatings produced on samples of 7075 aluminum alloy were studied and compared with those of samples treated with more commercial treatments, such as traditional anodizing and painting, and untreated ones. After the treatments, the different samples were characterized through scanning electron microscope (SEM) observations. The antifouling tests were carried out immersing the different coated samples in the Piave river for a month, collecting one sample series every week. After the immersion test, to evaluate the colonization by microalgae, the samples were investigated through stereomicroscope, inverted light microscope, and SEM. Results showed that the addition of silver/copper particles in the electrolyte does not modify the PEO process, obtaining thick and adherent coatings that contain particles both inside and outside of the pores. As regards the antifouling properties, surface PEO treated with copper particles exhibited a good effect inhibiting the colonization by microalgae.

1. Introduction

The appearance of aluminum alloys as an alternative material in boat and ship constructions is related to the 1960's (Holtyn, 1966) and, since then, aluminum is recognized as an advantageous material in shipbuilding by marine engineers and naval architects. In particular, it finds application in small boats as police or patrol boats, fishing vessels, fire boats or fast passenger vessels as catamarans (up to 400 passengers) in Europe, North America and especially in Asia (Allan, 1997). The lightweight, superior mechanical properties and corrosion resistance of aluminum alloys has dictated their use in many of these applications. Using aluminum, naval architects can design ships and boats with high-speed capability, long life, high payloads and low maintenance costs, as well as a high recycle value (Holtyn, 1972). The low density of aluminum, combined with high strength, toughness, and corrosion resistance, allow vessel designers to achieve weight savings of 15–20% over steel or composite designs (ASM International, 2017a; ASM International, 2017b). Weight savings equate to higher speed, increasingly demanded for vessels such as ferries, patrol boats, military craft, hydrofoils, fishing vessels, cargo vessels, leisure craft, and work boats.

The weight saving improves the ship stability allowing design of narrower ships (Brown, 1999). However, aluminum structures in marine environment suffer of some corrosion problems especially connected with fouling (Davis, 1999).

Biofouling is a common problem on man-made objects submerged in the waters throughout the world (Satheesh et al., 2016; Wang et al., 2016). The biofouling growth on a substrate in the aquatic environment is a complex process, which consists in the first moments in a binding of glycoproteins, polysaccharides and proteoglycans, dissolved in the water, followed by an initial biofilm formation, constituted by bacteria, protozoa, and microalgae, through the secretion of adhesive extracellular polymeric substances (EPS) (Mejdandžić et al., 2015). The colonization proceeds with the final settlement of invertebrate larvae and algal spores (Wahl, 1997; Maki, 2002).

Biofouling on submerged surfaces in the marine environment has considerable ecological and economical importance, besides particularly serious implications for shipping, offshore aquaculture, and coastal industries (Gerhart et al., 1988; Armstrong et al., 2000; Cassé and Swain, 2006; Qi et al., 2008; Patil and Anil, 2015). The effects are mainly due to the loss of productivity in aquaculture (De Nys and

* Corresponding author.

** Corresponding author.

E-mail addresses: pietrogianni.cerchier@studenti.unipd.it (P. Cerchier), lucapezzato@virgilio.it (L. Pezzato), emanuela.moschin@unipd.it (E. Moschin), marjorie.olivier@umons.ac.be (M.G.M. Olivier), isabella.moro@unipd.it (I. Moro), maurizio.magrini@unipd.it (M. Magrini).

Guenther, 2009) or increased costs of fuel to shipping, as well as the costs associated with ongoing prevention, management and control (Callow and Callow, 2002; Jackson, 2008). Therefore, the use of anti-fouling coatings in the marine environment has a long history. In particular, often organic coatings containing metallic species working as antifouling species are produced (Tang and Cooney, 1998; Chambers et al., 2006). The majority of tin-free antifouling paints currently available contain copper (Cao et al., 2011).

Organic coatings containing copper are already described in literature and the mechanism of action as antifouling compound is due to release of copper ions (Nirvan et al., 1982; Moreton, 1986; Callow, 1990; Del Amo et al., 1990; Ashraf and Edwin, 2016).

Moreover, even though the high cost of silver prevents its extensive application, the antifouling properties of organic coatings containing silver, as well as silver nanocomposites, have been recently studied (Neser and Kacar, 2010; Liu et al., 2014; Szabó et al., 2014; Selim et al., 2015). Elementary silver, in detail, is believed to function as antimicrobial either as a release system for silver ions or as contact-active material (Ho et al., 2004).

Nowadays, one of the most promising techniques to produce coatings that can improve the corrosion resistance of aluminum alloys is the Plasma Electrolytic Oxidation (PEO) (Song and Atrens, 2003). PEO, also called 'Microarc Oxidation (MAO), is a relatively novel surface modification derived from traditional anodizing, but working at higher current densities and potential. This treatment produces a protective oxide ceramic coating on the metallic surfaces (Jiang and Wang, 2010; Li et al., 2013). Many works can be found in literature regarding the improved corrosion performances by PEO coated aluminum alloys in different environments (Hosseini and Mehdi, 2014; Xiang et al., 2015; Venugopal et al., 2016). However, no works in literature exist regarding the antifouling properties of PEO coated samples even though, as reported above, the use of aluminum alloys in marine environments is widespread.

In this study the behavior of this new coating in a natural environment like Piave river was studied for the first time, with particular attention whether the coating can improve corrosion or antifouling properties of the aluminum alloy. This study represents a preliminary survey focused mainly on the antifouling effects of the PEO treatment.

In fact, the antifouling properties of different PEO coatings produced on samples of 7075 aluminum alloy, immersed in the estuarine Piave river for four weeks, were investigated through the analyses of the microalgal coverage developed on the substrates. In particular, coatings without additives and coatings containing silver or copper particles, incorporated in the PEO coatings directly during the production process, were tested. Moreover, different substrates without PEO (uncoated sample, an abrasive blasting sample, a conventionally anodized sample, and a sample with a commercial antifouling painting) were also tested as a comparison.

2. Materials and methods

2.1. PEO coating preparation

The different coatings were all produced on 7075 aluminum alloy. The nominal composition of the alloy is reported in Table 1.

Before PEO treatment, the samples were polished following standard metallographic techniques and then degreased using acetone through ultrasound. The PEO electrolyte was constituted by an aqueous alkaline solution with 5 g/l of NaOH and 25 g/l of Na₂SiO₃.

Table 1
Chemical composition of 7075 aluminum alloy.

| Al% | Mg% | Zn% | Cu% | Others% |
|------|-----|-----|-----|---------|
| 90.7 | 3.1 | 4.1 | 0.9 | 1.2 |

The plasma electrolytic oxidation process was carried out using a TDK-Lambda DC power supply of 300 V/8A capacity. During the treatment, the sample worked as anode and the cathode was a carbon steel mesh immersed in the electrolyte. The treatments were performed maintaining a constant current and letting the potential free to vary. The current density used was 0.3 A/cm² and the treatment lasted 5 min.

Among the coated samples, traditionally anodized ones were also tested as comparison. For this treatment, it was used a current density of 0.016 A/cm² for 25 min in a solution of sulfuric acid 20% using a lead cathode. The temperature of the electrolyte was maintained constant at 18 °C by a thermostatic bath. Other samples were painted: painting was performed sandblasting the samples and laying on the samples first one primer coat of epoxy resin and then two coats of white antifouling painting.

The silver and copper powders were appositely synthesized by hydrometallurgical processes and had average dimension of 0.5 μm and 3 μm respectively, as can be observed in Fig. S1.

These powders were added directly into the electrolyte during the treatments. The concentration of copper and silver in the coatings are respectively 0.8 mg/cm² and 0.3 mg/cm². Moreover, on the PEO treated samples, a sealing treatment was performed by immersing the samples into boiling water for 15 min.

The samples with copper or silver powders into the coatings were sealed using water added with other copper or silver powders, in order to increasing the amount of particles on the surfaces of the coatings.

After all the samples were coated, one per type was accurately characterized. To achieve this, the samples were first washed with deionized water and ethanol and dried with compressed air. The cross-sections of the treated samples were then cut and mounted in epoxy resin and polished with standard metallographic technique. Both the surface and the cross-section of treated samples were examined by a Cambridge Stereoscan 440 scanning electron microscope (SEM), equipped with a Philips PV9800 Energy Dispersive X-ray Spectroscopy (EDS), to evaluate the morphological features, the thickness of the coating and the elemental composition. The phase analysis was carried out through a Siemens D500 X-ray diffractometer using a nickel-filtered Cu Kα radiation source (λ = 0.15405 nm).

2.2. Antifouling test

After the characterization, seven types of samples, in quadruplicate, were prepared to perform the test for the evaluation of the antifouling properties of the coatings. During the test, all of replicated samples were completely immersed at the 40 cm depth in the Piave river.

The sampling site selected for the test (45.582065 N; 12.652398 E) is near to the river mouth, where the river is deep and tidal action is present. However, the test was performed in late spring, when the river flow is enough to prevent the ascent of the salt wedge. Every week, one series of samples was collected so up to four weeks and fixed with formalin neutralized with hexamethylentetramin. Moreover, the water pH and temperature were measured at every sampling. The test site and physical data are reported in Fig. 1.

2.3. Assessment microalgal colonization

At the beginning, fouling colonization was observed by a Zeiss Stemi 2000-c stereomicroscope. Moreover, to estimate the qualitative microalgal composition, the blocks were scraped by a blade into distilled water and the scraped material was then concentrated in a settling chamber. The microflora samples were observed at a Leitz Diavert inverted microscope. Microalgae were identified using standard keys, in particular for diatoms Peragallo and Peragallo (1897–1908), Husted (1930–1966), and Van der Werff & Hulls (1957–1974) were used as reference.

In addition, observations at scanning electron microscope were carried out to identify small microalgae, not detectable at light



Fig. 1. Image of the place selected for the antifouling tests with the samples immersed in the river water. In the table on the bottom left are reported the pH and temperature values recorded at the four sampling times.

microscope. Post-fixed blocks were dehydrated in a graded ethanol series, dried at critical point by a Polaron CPD7501, and coated with gold by an Edwards S 150B Sputter Coater. Then they were examined through a JEOL JSM-6490 scanning electron microscope.

2.4. Corrosion resistance

The most promising samples in terms of antifouling properties were tested in term of corrosion resistance with Scanning Vibrating Electrode Technique (SVET). SVET was applied to verify if the copper microparticles present in the PEO coating could induce the corrosion of the adjacent aluminum alloy matrix due to the formation of local galvanic couplings. For this purpose, both PEO-coated AA7075 samples (in the presence and absence of copper microparticles) were mounted in epoxy resin and their cross-sections were exposed by means of mechanical grinding (SiC paper up to the 2000 grade). Prior to the SVET measurements, the surfaces were rinsed with ethanol, distilled water and then dried with compressed air. The commercial equipment employed was the Uniscan SCV370 equipped with a Pt probe ($\varnothing = 50 \mu\text{m}$). The following operational parameters were employed: probe-sample distance equal to $180 \mu\text{m}$; vibration amplitude equal to $25 \mu\text{m}$ (peak-to-peak); scan speed equal to $500 \mu\text{m/s}$; step size equal to $50 \mu\text{m}$; and a sensitivity equal to $800 \mu\text{V}$. The scanned area varied between $12 \times 48 \text{ mm}^2$. The tests were performed in near-neutral aerated 12.00 mM NaCl solution (Coelho et al., 2016) ($\text{pH} \approx 6$, conductivity, $k \approx 1300 \mu\text{S cm}^{-1}$, volume $\approx 800 \text{ mL}$). Each measurement had a total duration of 3 h (comprising 6 consecutive scans) and it was repeated twice.

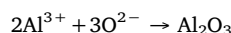
3. Results and discussion

3.1. Surface characterization

The PEO coating without additives was produced working at high current densities and short treatment times and the complete characterization of the PEO treated sample is reported in (Pezzato et al., 2016). The stereomicroscope observation of the surfaces of the samples treated with silver and copper particles in the electrolyte can be observed respectively in Fig. 2a and 2bb. Moreover, the coating seemed to

be not influenced by the presence of the particles and resulted continuous and homogeneous with the typical grey color of the PEO coatings produced on aluminum alloys.

During PEO process the oxidation of aluminum takes place:



However, this electrochemical reaction is not the only one contributing to the coating formation, as there is also codeposition of other species from electrolytic bath and the formation of different oxides (Walsh et al., 2009).

The EDS analysis at SEM of the coatings containing silver or copper powders revealed the presence of particles both on the surface and inside of the pores characterizing PEO coatings (Fig. 3). The presence of the particles into the electrolyte seemed not to influence the formation and the morphology of the coatings, which was almost the same if compared with that obtained without particles (Fig. 3a and b). In detail, it can be observed the typical surface of PEO coatings rich of pores and micro-cracks (Fig. 3a, c and 3e) and the thickness of the coatings is between 15 and $20 \mu\text{m}$ (Fig. 3b, d and 3f). Analysis of the cross section of the samples highlighted also the typical double layer structure of PEO coatings, with an inner thin and dense layer, called also barrier layer, and an external porous layer, called technological layer (Jiang and Wang, 2010). Moreover, from the surface observation, the pores resulted partially sealed by the sealing treatment in boiling water. EDS analysis of the white spots, observed at SEM in backscattered electron mode, revealed that these spots correspond to the silver (Fig. 3g) and copper particles (Fig. 3h). From the semi-quantitative EDS analysis, performed on the cross section of the samples, areas without the particles did not show remarkable differences in the composition: aluminum and silicon compounds with oxygen (Table 2). Moreover, the composition of the coating is not influenced by the presence of the particles and it is in accordance with the composition of the electrolyte and substrate.

X-ray diffraction (XRD) analyses were performed on the samples containing silver or copper particles in order to identify the different phases of the coatings (Fig. S2). The diffraction pattern was also compared with that obtained on the sample treated without silver or copper particles, reported in Pezzato et al. (2016).

Both analyses, besides the peaks of silver and copper in the different

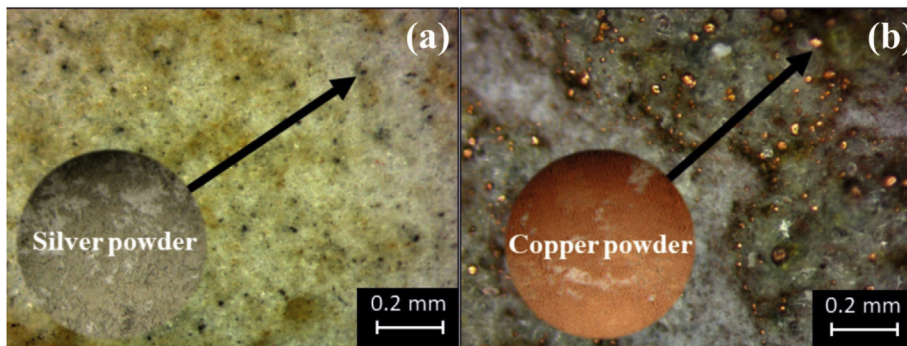


Fig. 2. Image of the two PEO coatings obtained with silver (a) and copper (b) powder. The particles are clearly visible on the surfaces.

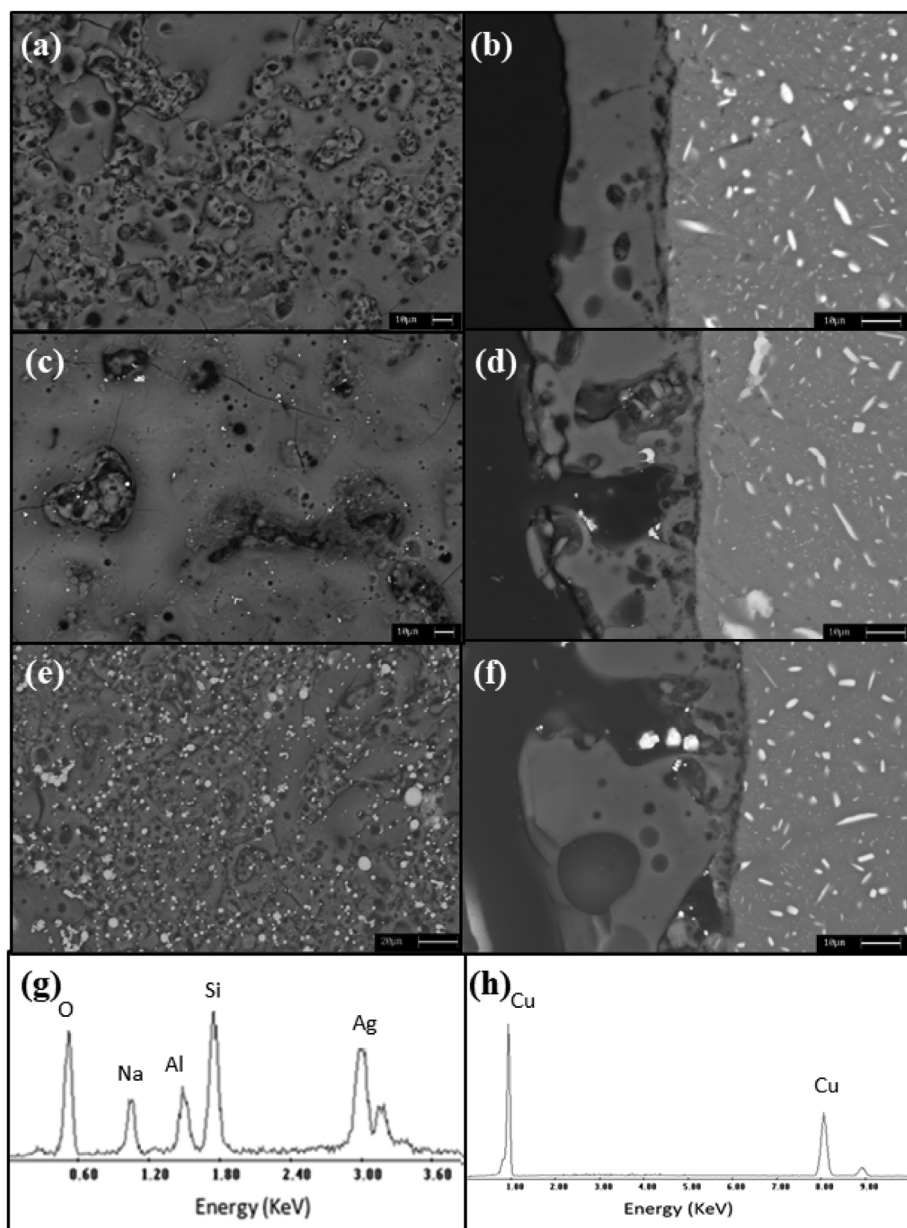


Fig. 3. Image of the surface and section of the PEO coatings with and without silver and copper powders. (a) surface of sample without particles; (b) section of sample without particles; (c) surface of sample with silver; (d) section of sample with silver; (e) surface of sample with copper; (f) section of the sample with copper; (g) EDS analysis of the silver particles; (h) EDS analysis of the copper particles.

Table 2
EDS semi-quantitative analysis performed on the cross section of the samples.

| Sample | O% | Al% | Si% |
|--------------|----|-----|-----|
| PEO | 38 | 22 | 40 |
| PEO + Silver | 44 | 18 | 38 |
| PEO + Copper | 41 | 20 | 39 |

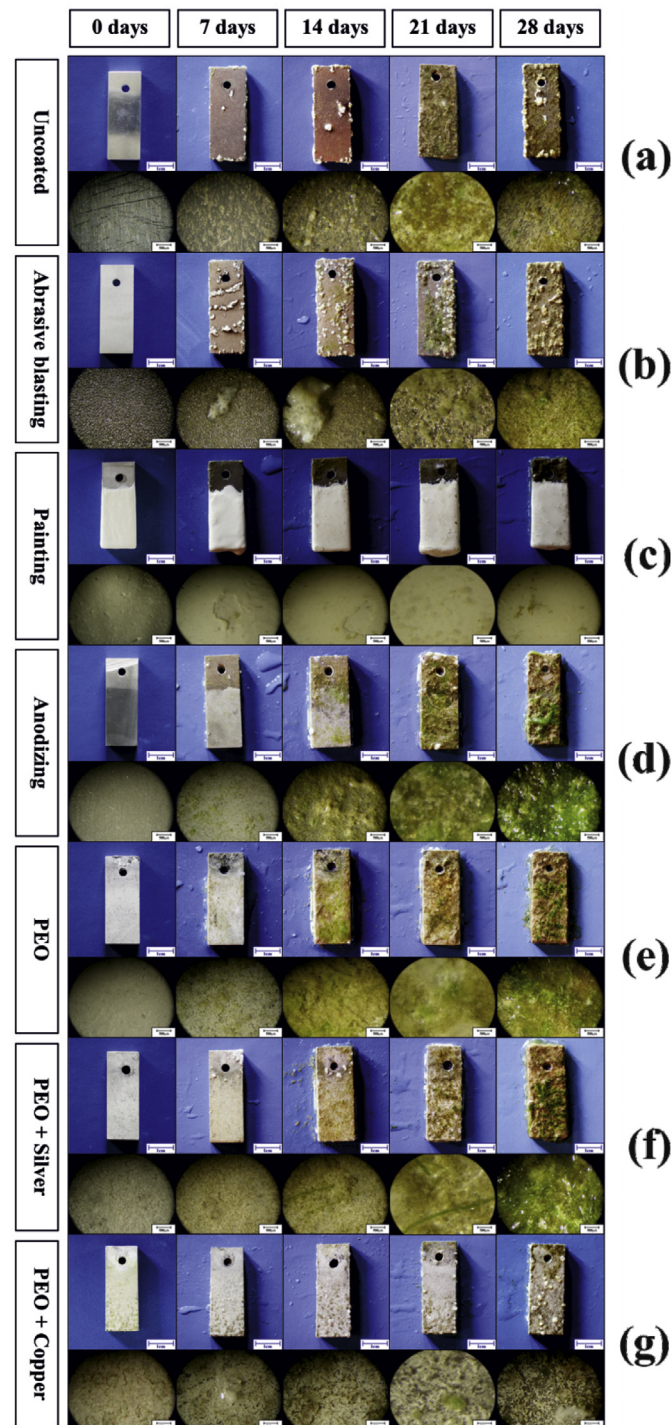


Fig. 4. Image of the samples used for the antifouling test.

coatings, showed the peaks of Al_2O_3 and Al_2SiO_5 in agreement with the composition of the alloy and the electrolyte of the PEO process.

3.2. Fouling analysis

The samples and their observation at the stereomicroscope during the antifouling test were shown in Fig. 4.

As it can be observed, the uncoated and abrasive blasting samples after 28 days exhibited the presence of white oxide spots on the surfaces, as expected in the absence of any protective coating (Fig. 4a and b). These white spots are in fact due to corrosion phenomena on the aluminum surface. Moreover, as predictable, the oxidation was more remarkable in the case of sand blasting of the surface, since a greater area was exposed to the water. As regards the colonization by the foulers, the surfaces showed a similar behavior: in fact, even if on one hand the surface roughness, due to the blasting, promotes the settlement of the organisms, on the other hand the higher oxidation, probably due to the substrate dissolution and the release of aluminum ions, could have negative effects on the microalgal adhesion (Gensemer and Playle, 1999).

The commercial antifouling painting treatment on aluminum alloy (Fig. 4c) resulted to have great antifouling and anticorrosive effects, since the surface did not change after the four weeks of immersion and no trace of foulers nor corrosion was detected. The antifouling painting used was a so-called “hard” bottom paint and it is typically applied to fast ships. It differs from other kinds of paintings, like abrasive ones, whose coating gradually wear away releasing the biocide, containing copper oxide particles, and therefore its antimicrobial activity is caused only by chemical action (Almeida et al., 2007). In the case of its application to aluminum alloys, a primer under the paint is necessary in order to avoid galvanic couple and rapid corrosion of the less noble metal (Almeida et al., 2007). The presence of the biocide inside the paint together with the smoothness of the surface allows to the sample to have the greatest antifouling effect.

Even if the anodized sample seemed abundantly colonized already after 21 days (Fig. 4d), at the fourth week, the three samples anodizing (Fig. 4d), PEO coating (Fig. 4e) and PEO coating with silver (Fig. 4f) showed a similar fouling coverage. In particular, it seems that, despite the improved corrosion resistance of these samples in comparison with untreated aluminum alloy, their ceramic coatings offer a substrate more favorable to the settlement of the foulers, due to their chemical inertness. This fact is also connected with the porosity of the PEO surface, because the pores are ideal zones for the colonization of different species, indeed is reported in literature the use of PEO coating as substrate for cell growth (Whiteside et al., 2010). The presence of silver seemed to not increase the antifouling effect of the coating that resulted similar to anodizing PEO samples (Fig. 4f). This fact can be linked with the concentration of silver inside of coating, which was probably not enough to produce an appreciable effect. In detail, for these three treatments, the presence of colonization can be clearly detected already after 14 days of immersion (Fig. 4e and f). However, the presence of the coating remarkably increases the corrosion resistance of the samples, in fact no white oxide spots were detected both in the anodized and PEO coated samples.

On the contrary, the PEO coating with copper powder (Fig. 4g) showed a remarkable antifouling effect. In fact, only after 28 days a weak presence of organisms could be observed. Also the corrosion phenomena on the other treated samples were less than on the untreated sample.

Therefore, the sample treated with PEO containing copper particles seemed the most promising in order to produce a surface with good antifouling properties and corrosion resistance, useful for example as substrate for commercial paintings. In this way, in fact, the presence of cracks in the painting will not be deleterious for the aluminum substrate both in term of corrosion and antifouling resistance.

In this study all tested substrates were immersed and exposed to the

Table 3

Relative abundance of chlorophycean filaments and diatoms on the different samples during the experimental period (“–” = absent; “C or D” = low; “CC or DD” = high; “CCC or DDD” = very high).

| | 7 days | 14 days | 21 days | 28 days |
|-------------------|--------|-----------|---------|-----------|
| Uncoated | D | D + C | C + DDD | CC + DDD |
| Abrasive Blasting | – | DD | DDD | DDD + CC |
| Painting | – | – | – | – |
| Anodizing | DD | DDD + C | DD + CC | DD + CCC |
| PEO | DDD | DDD + CCC | DD + CC | DDD + CCC |
| PEO + Silver | DD | DDD + CC | DD + C | DD + CCC |
| PEO + Copper | D | D | D | DD + C |

same biological, chemical, physical, and hydrodynamic conditions, therefore differences in the colonization by microphytobenthos are due only to the diverse coatings.

Concerning the microfouling community, in order to estimate the surface colonization, microscopic analysis of the samples was performed, through the identification of the different settled organisms and their contribution to the sample coverage. The data reported in Table 3 highlighted that the colonization was ascribable to diatoms and chlorophycean filaments.

Colonization analyses, carried out by light and scanning electron microscope (Figs. 5 and 6) showed that in all tested samples, except painting, the developed microfouling communities were dominated by benthic diatoms. These photosynthetic microorganisms, together with bacteria and cyanobacteria, are in fact the major constituents of biofilm on submerged surfaces (Callow and Callow, 2002; Patil and Anil, 2015).

The main genera of benthic diatoms, observed in all tested coatings, were represented by pennate species, characterized by a bilateral symmetry: *Navicula* Bory, *Nitzschia* Hassall, *Surirella* Turpin, and

Tabularia (Kutzing) D.M. Williams & Round. Only two centric diatom taxa, belonging to the genus *Melosira* Agardh, characterized by cells, united in colonies forming filaments attached to the substrate, were recorded. The dominance of pennate diatoms over centric ones in a biofilm is due to the presence of structures (raphe or pores) for the secretion of adhesive extracellular polymeric substances (EPS), which enhance their attaching and gliding capability on a substrate (Molino and Wetherbee, 2008; Gomathi Sankar et al., 2015). This result is in agreement with data reported by Patil and Anil (2015) on population of fouling diatoms in non-toxic and toxic substrates, where pennate diatoms were dominant in terms of abundance and number of species.

Filamentous chlorophyceans also appeared, from the second week reaching high density at the fourth week (Figs. 4, 5l and 6d, and h; Table 3). Sometimes, the presence of these last ones prevented observation, identification, and quantification of small diatom species, established on substrates, causing a biodiversity underestimation. Then again, diatom biofilms represent an important step for the subsequent attachment by other fouling organisms (Patro et al., 2012).

Uncoated and abrasive blasting samples, during the first and second weeks, showed the surface covered by inorganic deposit (Fig. 5a and e) and a weak colonization by sessile diatoms, such as *Tabularia fasciculata* (Agardh) D.M. Williams & Round (Fig. 5b) and *Melosira varians* Agardh; while starting from the third week the surfaces of these samples appeared colonized also by chlorophycean filaments (Fig. 5c) and vagile diatoms (i.e. *Amphora* spp. and *Nitzschia* spp.) (Fig. 5g). After 28 days of immersion the coverage was very abundant (Table 3; Fig. 5d and h). The painting treatment, instead, resulted uncovered by foulers during all the tested period (Table 3; Fig. 4).

Anodizing sample since the first week showed a high colonization by diatoms (Fig. 5i), that after 14 days increased both as the species biodiversity and as cell density (Fig. 5j and k). Chlorophycean filaments

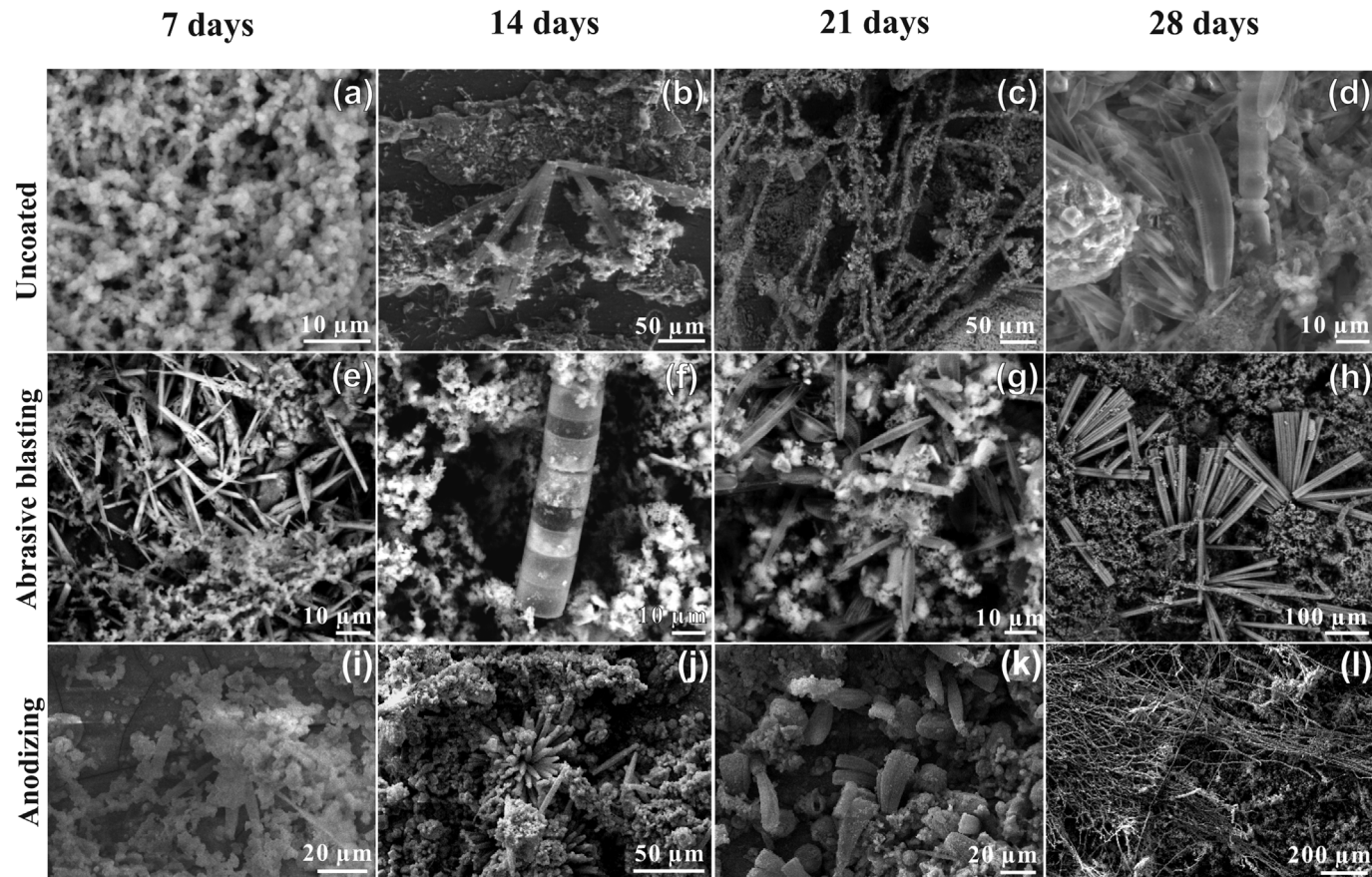


Fig. 5. Scanning electron micrographs of the Uncoated (a–d), Abrasive blasting (e–h), and Anodizing (i–l) samples during the antifouling test (7, 14, 21, and 28 days).

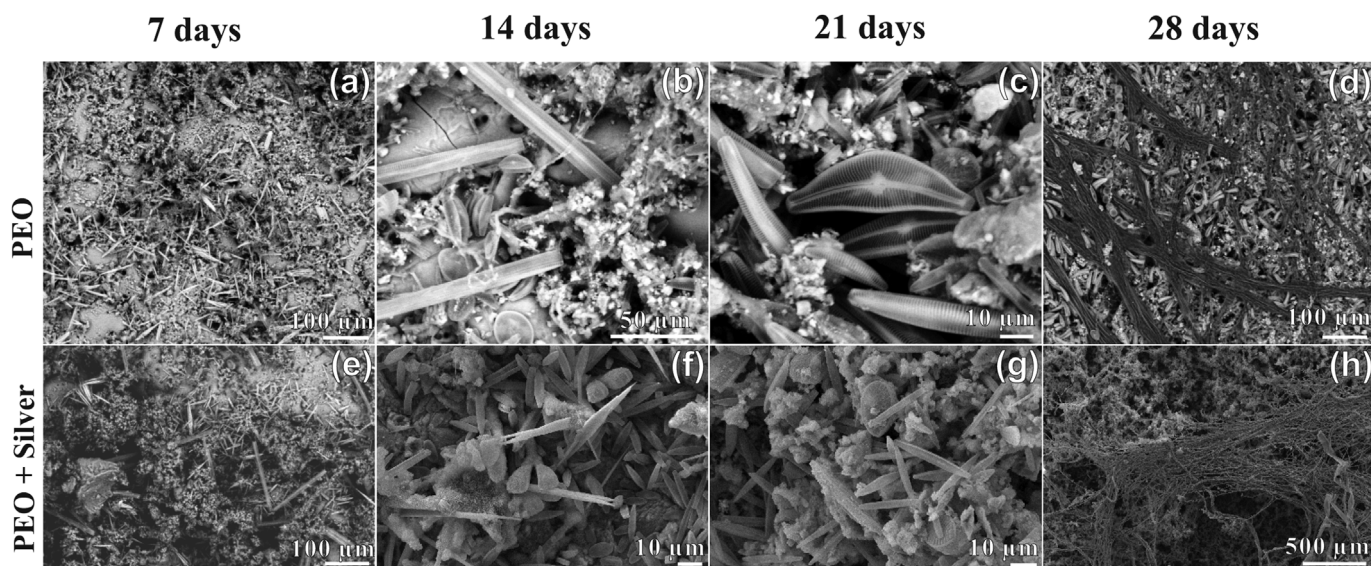


Fig. 6. Scanning electron micrographs of the PEO (a–d) and PEO + Silver (e–h) samples during the antifouling test (7, 14, 21, and 28 days).

appeared during the second week (Table 3) and increased in the following weeks, up till dominated the microalgal community after 28 days (Fig. 5l).

PEO coating samples (Fig. 6a and d; Table 3) showed a high coverage ascribable to many species. In particular, pennate diatoms, both sessile and vagile, belonging to the genera *Cocconeis* Ehrenberg, *Synedra* Ehrenberg, *Amphora* Ehrenberg ex Kützinger, *Cymbella* Agardh, and *Rhoicosphenia* Grunow (Fig. 6b and c), contributed to the high biodiversity. In addition, chlorophyceans were present as packed filaments, establishing a living substrate suitable to other microalgal colonizers (epiphytes) (Fig. 6d).

PEO + silver powder coating samples showed coverage slightly lower than PEO ones both in species number and in abundance (Table 3). In particular, since the first week a colonization by diatoms, mainly characterized by stalked taxa, has been observed (Fig. 6e); after 14 days the species diversity and their abundance increased (Fig. 6f; Table 3). A slightly decrease was observed at the third week, with the presence of inorganic precipitates (Fig. 6g). After 28 days, chlorophycean filaments increased such that they dominated diatoms (Fig. 6h; Table 3).

It is interesting to observe that after 21 days of immersion, both PEO and PEO + silver coating samples showed a slightly decrease in the fouling colonization and a following recovery of the coverage at the fourth week, both by diatoms and by chlorophyceans (Table 3). This could be due to a faster water river flow, causing the detachment of the peduncolate taxa, weakly attached to the substrate.

The comparison between the PEO + silver and PEO treatments, showing in both cases a various microalgal community, suggests that the silver content may be not enough to determine a strong antifouling effect.

Regarding the PEO + copper treatment, as already highlighted in the analysis of Fig. 4g, the presence of copper in the treatment delayed the colonization by microalgae, as evidenced from the light microscope analysis (Table 3). During the experimental test the microphytobenthos community was very poor, with slight increase only after 28 days. This result leads us to believe that treatment with PEO + copper has good antifouling properties, as expected since it is known that copper-based antifouling paints have been used to combat marine fouling (WHOI, 1952; Brady, 2000).

3.3. Corrosion resistance

In order to understand if the particles could produce problems of

galvanic corrosion with the substrate the most promising sample in term of antifouling resistance (the PEO + copper one) was tested with SVET. As comparison was also tested the cross-section of the PEO-coated sample after the SVET test and the corresponding SVET maps obtained between 30 and 110 min of immersion. First, it can be seen that the alloy is subjected to a local anodic attack, as depicted by the arrows in Fig. S3b. This result illustrates the susceptibility of the alloy to localize corrosion as a result of the presence of intermetallics. The centers of anodic activity seemed to develop at random locations, as suggested by the different performed scans (here not shown). The corresponding cathodic activity appears spread over the entire alloy surface and cannot be assessed with precision. From the scan performed along the entire inferior border (Fig. S3c), no significant electrochemical activity could be observed on the alloy part. In fact, the spatial resolution of SVET is often not great enough to detect local activity arising from individual intermetallics/pits (Williams et al., 2010; González-García et al., 2011). For that reason, the spatial assignment of corrosion in such systems is a matter of probability. In other words, since localized corrosion events are time-dependent, the probe scanning over a certain point can only detect activities that take place there at that exact moment.

The sample comprising the PEO coating containing copper microparticles showed similar results (Fig. 7). The SVET map obtained from the center of the alloy (Fig. 7b) once again indicates the occurrence of anodic attack. In this case, the scan performed along the border (Fig. 7c) could eventually depict clear centers of anodic activity. In general, these centers appear to be established in space and time randomly. The difference in the intensity of the anodic peaks observed between Fig. S3 and Fig. 7 is not necessarily reflective of distinct corrosion rates. Once again, localized phenomena measured by SVET cannot be quantitatively compared, since the probe is necessarily losing information while scanning the surface in a point-by-point fashion.

In conclusion, for both coated systems, SVET was able to highlight the behavior of an alloy prone to localized corrosion. Furthermore, galvanic coupling between the copper microparticles from the PEO coating and the aluminum matrix does not seem to be the driving force for the corrosion of the alloy. Otherwise, the anodic activity should be preferentially located near the borders of the matrix, next to the referred PEO coating. It is worth mentioning that these SVET outcomes do not prove a complete absence of local galvanic coupling related to the coating doped with copper. Instead, they prove that the anodic attacks induced by the alloy constituent intermetallics are considerably

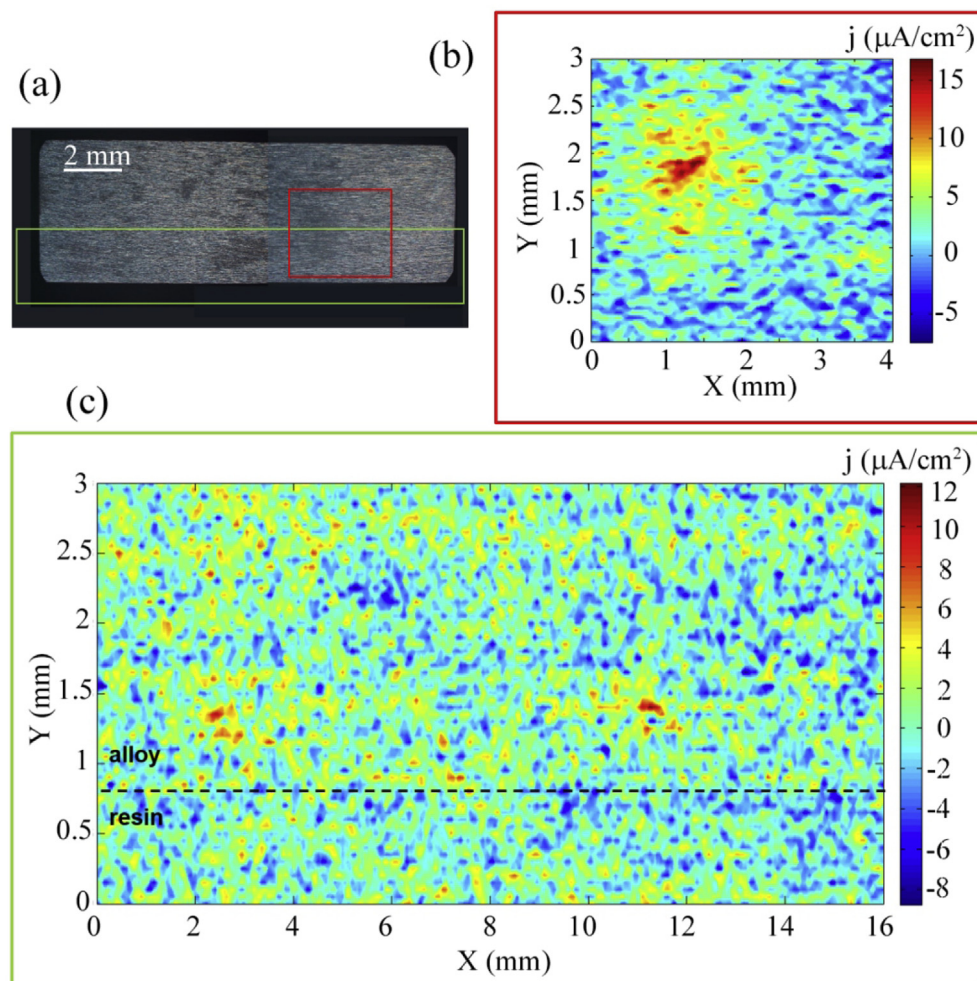


Fig. 7. (a) The resulting cross-section of the PEO + Cu particles-coated AA7075 after 3 h of immersion in 12.00 mM NaCl electrolyte. The corresponding time-dependent current density maps obtained by SVET (b) from 110 to 120 min and (c) from 30 to 80 min of exposure.

stronger than an eventual galvanic corrosion process promoted by the PEO coating.

4. Conclusions

The results show that all the treated samples are characterized by higher corrosion resistance if compared with the untreated ones. Anodizing and PEO coating without particles or with silver particles are however very prone to fouling and are colonized faster in comparison with uncoated or abrasive blasting aluminum alloy. The surface PEO treated with copper particles actually exhibits good antifouling effect and SVET analysis reveals that the presence of the particles does not produce galvanic corrosion of the substrate. However, best performance in term of antifouling effect is given by the commercial paintings. The use of this kind of paintings however has problems in the presence of ruptures in the varnish, and as a consequence, optimum solution probably can be achieved combining copper-containing PEO coating with varnish in order to give to the sample good corrosion and fouling resistance even in presence of some cracks in the varnish.

Acknowledgment

This work was supported by grants provided by the Scientific Research Grant (EX 60%) of the University of Padova, Italy.

Appendix A. Supplementary data

Supplementary data related to this article can be found at <http://dx.doi.org/10.1016/j.ibiod.2018.06.005>.

References

- Allan, R.G., 1997. Applications for aluminum alloys in the marine industry a current perspective. In: Proceedings of Alumitech, Atlanta, 20–23 May, 1997, pp. 292.
- Almeida, E., Diamantino, T., de Sousa, O., 2007. Marine paints: the particular case of antifouling paints. *Prog. Org. Coating* 59, 2–20.
- Armstrong, E., Boyd, K., Pisacane, A., Peppiatt, C., Burgess, J., 2000. Marine microbial natural products in antifouling coatings. *Biofouling* 16, 215–224.
- Ashraf, P.M., Edwin, L., 2016. Nano copper oxide incorporated polyethylene glycol hydrogel: an efficient antifouling coating for cage fishing net. *Int. Biodeterior. Biodegrad.* 115, 39–48.
- ASM International, 2017a. ASM Handbook Vol. 2. Properties and Selection: Nonferrous Alloys and Special-purpose Materials.
- ASM International, 2017b. ASM Handbook Vol. 13B. Corrosion: Materials.
- Brady Jr., R.F., 2000. No more tin, what now for fouling control. *J. Prot. Coatings Linings* 5, 42–46.
- Brown, S., 1999. Feasibility of Replacing Structural Steel with Aluminum Alloys in the Shipbuilding Industry. University of Wisconsin-Madison.
- Callow, M., 1990. Ship Fouling. Problems and Solutions, vol. 5. Chemical Industries, London, pp. 123–127.
- Callow, M.E., Callow, J.A., 2002. Marine biofouling: a sticky problem. *Biologist* 49, 1–5.
- Cao, S., Wang, J., Chen, H.S., Chen, D., 2011. Progress of marine biofouling and antifouling technologies. *Chin. Sci. Bull.* 56, 598–612.
- Cassé, F., Swain, G.W., 2006. The development of microfouling on four commercial antifouling coatings under static and dynamic immersion. *Int. Biodeterior. Biodegrad.* 57, 179–185.
- Coelho, L.B., Mouanga, M., Druart, M.-E., Recloux, I., Cossement, D., Olivier, M.-G., 2016.

- A SVET study of the inhibitive effects of benzotriazole and cerium chloride solely and combined on an aluminium/copper galvanic coupling model. *Corrosion Sci.* 110, 143–156.
- Chambers, L., Stokes, K., Walsh, F., Wood, R., 2006. Modern approaches to marine antifouling coatings. *Surf. Coating Technol.* 201, 3642–3652.
- Davis, J.R., 1999. *Corrosion of Aluminum and Aluminum Alloy*. ASM International.
- De Nys, R., Guenther, J., 2009. The impact and control of biofouling in marine finfish aquaculture. In: Hellio, C., Yebra, D. (Eds.), *Advances in marine Antifouling Coatings and Technologies*. Cambridge, pp. 177–221.
- Del Amo, B., Giudice, C., Villoria, G., 1990. Evaluating anti-fouling paints. *Eur. Coating J.* 1, 8–14.
- Geneser, R.W., Playle, R.C., 1999. The bioavailability and toxicity of aluminum in aquatic environments. *Crit. Rev. Environ. Sci. Technol.* 29, 315–450.
- Gerhart, D., Rittschof, D., Mayo, S., 1988. Chemical ecology and the search for marine antifoulants. Studies of a predator-prey symbiosis. *J. Chem. Ecol.* 24, 1905–1917.
- Gomathi Sankar, G., Sathya, S., Sriyutha Murthy, P., Das, Arindam, Pandiyan, R., Venugopalan, V.P., Mukesh, Doble, 2015. Polydimethyl siloxane nanocomposites: their antifouling efficacy in vitro and in marine conditions. *Int. Biodeterior. Biodegrad.* 104, 307–314. <http://dx.doi.org/10.1016/j.ibiod.2015.05.022>.
- González-García, J.M.C., Mol, T., Muselle, I., De Graeve, G., Van Assche, G., Scheltjens, G., Van Mele, B., Terryn, H., 2011. A combined mechanical, microscopic and local electrochemical evaluation of self-healing properties of shape-memory polyurethane coatings. *Electrochim. Acta* 56, 9619–9626.
- Ho, C., Tobis, J., Sprich, C., Thomann, R., Tiller, J., 2004. Nanoseparated polymeric networks with multiple antimicrobial properties. *Adv. Mater.* 12, 957–961.
- Holtyn, C., 1966. Aluminum - The age of ships. *Soc. Nav. Archit. Mar. Eng.* 356–391.
- Holtyn, C.H., 1972. The construction and service record of a 306 Ft. Aluminum trailer-ship. *Soc. Nav. Archit. Mar. Eng.*
- Hossein, F., Mehdi, J., 2014. Investigation on the corrosion behaviour and microstructure of 2024-T3 Al alloy treated via plasma electrolytic oxidation. *J. Alloy. Comp.* 604, 36–42.
- Hustedt, F., 1930-1966. Die Kieselalgen Von Deutschland, Österreichs Und der Schweiz Mit Berücksichtigung der Übrigen Länder Europas Sowie der Angrenzender Mehresgebiete. In: Rabenhorst's Kriptogamen-Flora Von Deutschland, Österreichs Und Der Schweiz, vol. 7 Akad; Verlag. M.B.H, Leipzig Tl. 2. 920 Pp.: Tl., 2 845 Pp.; Tl. 3, 816 pp.
- Jackson, L., 2008. Marine biofouling: an assessment of risks and management initiatives. In: *Global Invasive Species Programme*, pp. 1–68.
- Jiang, B., Wang, Y., 2010. Plasma electrolytic oxidation treatment on aluminum and titanium alloys. In: Dong, H. (Ed.), *Surface Engineering of Light Alloys*, Cambridge, pp. 110–180.
- Li, Q., Linag, J., Wang, Q., 2013. Plasma Electrolytic Oxidation coatings on lightweight metals. *Mod. Surf. Eng. Treat* 4, 75–99.
- Liu, T., Dong, Y., He, T.G., Zhang, F., 2014. Films with nanosilvers improve biocorrosion resistance of aluminum in sea water. *Surf. Eng.* 30, 6–10.
- Maki, J., 2002. Biofouling in the marine environment. In: *Encyclopedia of Environmental Microbiology*. Wiley & Sons, New York, pp. 610–619.
- Mejdandžić, M., Ivanković, T., Pfannkuchen, M., Godrijan, J., Pfannkuchen, D.M., Hrenović, J., Ljubešić, Z., 2015. Colonization of diatoms and bacteria on artificial substrates in the northeastern coastal Adriatic Sea. *Acta Bot. Croat.* 74 (2), 407–422.
- Molino, P., Wetherbee, R., 2008. The biology of biofouling diatoms and their role in the development of microbial slimes. *Biofouling* 24, 365–379.
- Moreton, B.B., 1986. Copper alloys in marine environments today and tomorrow- part II. *Corrosion Prev. Contr.* 33, 17–20.
- Neser, G., Kacar, A., 2010. The antifouling performance of gelcoats containing biocides and silver ions in seawater environment. *J. Coating Technol. Res.* 7, 139–143.
- Nirvan, Y., De, C.P., Kumar, D., 1982. Copper based antifouling paints for prevention of marine growth on ship Hulls. *Defence Sci. J.* 32, 55–66.
- Patil, J.S., Anil, A.C., 2015. Efficiency of copper and cupronickel substratum to resist development of diatom biofilms. *Int. Biodeterior. Biodegrad.* 105, 203–214.
- Patro, S., Adhavan, D., Jha, S., 2012. Fouling diatoms of Andaman waters and their inhibition by spinal extracts of the sea urchin *Diadema setosum*. *Int. Biodeterior. Biodegrad.* 75, 23–27.
- Peragallo, H., Peragallo, M., 1897-1908. *Diatomees Marine de France et des Districts Maritimes Voisins*. Micrographe Editeur Grez sur Loing (S. et M.), pp. 419.
- Pezzato, L., Brunelli, K., Dabalà, M., 2016. Corrosion properties of plasma electrolytic oxidation coated 7075 treated using an electrolyte containing lanthanum-salts. *Surf. Interface Anal.* 48, 729–738.
- Qi, S., Zhang, S., Yang, L., Qian, P., 2008. Antifouling and antibacterial compounds from the gorgonians *Subergorgia suberosa* and *Scrippearia gracillis*. *Nat. Prod. Res.* 22, 154–166.
- Satheesh, S., Ba-akdash, M.A., Al-Sofyani, L.A., 2016. Natural antifouling compound production by microbes associated with marine macroorganisms - a review. *Electron. J. Biotechnol.* 21, 26–35.
- Selim, M., El-Safty, S., El-Sockary, M., Hashem, A., Abo Elenien, O., EL-Saeed, A., Fatthallah, N., 2015. Modeling of spherical silver nanoparticles in silicone-based nanocomposites for marine antifouling. *RSC Adv.* 7, 63175–63185.
- Song, G., Atrens, A., 2003. Understanding magnesium corrosion—a framework for improved alloy performance. *Adv. Eng. Mater.* 5, 837–858.
- Szabó, T., Mihályb, J., Sajóc, I., Telegdia, J., Nyikosa, L., 2014. One-pot synthesis of gelatin-based, slow-release polymer microparticles containing silver nanoparticles and their application in anti-fouling paint. *Prog. Org. Coating* 7, 1226–1232.
- Tang, R., Cooney, J., 1998. Effects of marine paints on microbial biofilms development on three materials. *J. Ind. Microbiol. Biotechnol.* 20, 275–280.
- Van der Werff, A., Hulls, H., 1957-1974. *Diatomeeën flora Van Nederland*. Otto Koeltz Science Publishers, Koenigstein (Volum I, II, III).
- Venugopal, A., Srinath, J., Krishna, L., Narayanan, P., Sharma, S., Venkitakrishnan, P., 2016. Corrosion and nanomechanical behaviors of plasma electrolytic oxidation coated AA7020-T6 aluminum alloy. *J. Mater. Sci. Eng.* 660, 39–46.
- Wahl, M., 1997. Living attached: aufwuchs, fouling, epibiosis. In: Nagabhushanam, R., Thompson, M. (Eds.), *Fouling Organisms of the Indian Ocean: Biology and Control Technology*, New Delhi, pp. 31–84.
- Walsh, F.C., Low, C.T.J., Wood, R.J.K., Stevens, K.T., Archer, J., Poeton, A.R., Ryder, A., 2009. Plasma electrolytic oxidation (PEO) for production of anodised coatings on lightweight metal (Al, Mg, Ti) alloys. *Trans. Inst. Met. Finish.* 83, 122–135.
- Wang, G., Chai, K., Wu, J., Liu, F., 2016. Effect of *Pseudomonas putida* on the degradation of epoxy resin varnish coating in seawater. *Int. Biodeterior. Biodegrad.* 115, 156–163.
- Whiteside, P., Matykina, E., Gough, J., Skeldon, P., Thompson, G., 2010. In vitro evaluation of cell proliferation and collagen synthesis on titanium following plasma electrolytic oxidation. *J. Biomed. Mater. Res.* 94, 38–46.
- Williams, G., Coleman, A.J., McMurray, H.N., 2010. Inhibition of Aluminium Alloy AA2024-T3 pitting corrosion by copper complexing compounds. *Electrochim. Acta* 55, 5947–5958.
- Woods Hole Oceanographic Institution, United States. Navy Dept. Bureau of Ships, 1952. *Marine Fouling and its Prevention*; Prepared for Bureau of Ships, Navy Dept. <http://dx.doi.org/10.1575/1912/191>. <https://hdl.handle.net/1912/191>.
- Xiang, N., Song, R., Li, H., Wang, C., Mao, Q., Xiong, Y., 2015. Study on microstructure and electrochemical corrosion behavior of PEO coatings formed on aluminum alloy. *J. Mater. Eng. Perform.* 24, 5022–5031.